Journal of Controlled Release 361 (2023) 29–39

Contents lists available at ScienceDirect

Journal of Controlled Release

journal homepage: www.elsevier.com/locate/jconrel

Placental drug transport and fetal exposure during pregnancy is determined by drug molecular size, chemistry, and conformation

Katherine C. Fein [a], Mariah L. Arral [a], Julie S. Kim [a], Alexandra N. Newby [a], Kathryn A. Whitehead [a,b,*]

[a] Department of Chemical Engineering, Carnegie Mellon University, 5000 Forbes Ave, Pittsburgh, PA 15213, United States of America
[b] Department of Biomedical Engineering, Carnegie Mellon University, 5000 Forbes Ave, Pittsburgh, PA 15213, United States of America

ARTICLE INFO

Keywords:
Drug delivery
Maternal health
Fetal toxicity
Pregnancy
Placenta
Macromolecules
Physicochemical properties

ABSTRACT

Pregnant people are unable to take many prescription and over-the-counter medications because of suspected or known risk to the fetus. This undermedication contributes to the high maternal mortality rate in the United States and detracts from the quality of life of pregnant people. As such, there is an urgent need to develop safe pharmaceutical formulations for use during pregnancy. Most drugs are small molecules that easily cross the placenta, which is the biological barrier that separates the maternal and fetal bloodstreams. One potential approach to preventing fetal drug accumulation is to design drug compounds that are excluded by the placenta; however, there is little understanding of how macromolecular drug properties affect transplacental transport. To address this knowledge gap, we examined the transport behavior of fluorescently-labeled polymers with varying size, conformation, and chemistry. We compared these polymers to unconjugated fluorescein, a small molecule model drug that readily crosses biological barriers. We found that molecular size affected transplacental transport in an *in vitro* model, BeWo b30 monolayers, as well as in pregnant mice, with larger polymers having lower permeability. In addition to size, polymer chemistry altered behavior, with polyethylene glycol (PEG) molecules permeating the placental barrier to a greater extent than dextrans of equivalent molecular weight. PEG molecules were also more readily taken up into placental cells *in vivo*. These findings will inform the future development of drug conjugates or other macromolecular medicines that can safely be used during pregnancy.

1. Introduction

Up to 90% of pregnant people require medication during pregnancy, whether for a pre-existing condition or one developed while pregnant [1]. Despite this need, the effects of over-the-counter and prescription medications on fetal development are insufficiently studied and poorly understood. Many drugs are excluded from use during pregnancy, and even those historically considered safe during pregnancy are now being questioned, including acetaminophen, the all-purpose pain reliever recommended to pregnant women [2]. This lack of scientific evidence on medication use during pregnancy leads to inconsistent recommendations by clinicians and confusion among pregnant people about what is safe to use while pregnant. Ultimately, many people discontinue or reduce the dose of medications used pre-pregnancy or are unmedicated for pregnancy-induced conditions [3].

The crux of the problem is that most small molecules easily cross the placenta, which is the organ that develops during pregnancy to connect the maternal and fetal bloodstreams, acting as the barrier between them [4]. Recently, a potential solution to drug accumulation in the fetus has emerged in which small molecule drugs are incorporated into nanoscale carriers that limit transport across the placenta [5,6]. These nano approaches, which include dendrimer nanoparticles and PEG conjugation, retain the medication in the maternal compartment while preserving efficacy. While these studies have made important progress, widespread clinical adoption will require a better understanding of how the physicochemical properties of macromolecules affect interactions with and transport across the placenta.

The placenta comprises several layers of cells: the capillary endothelium lining the fetal blood vessels, a layer of cytotrophoblasts, and a layer of syncytiotrophoblasts that contact the maternal blood system. The syncytiotrophoblast layer serves as the major transport barrier [7]. Molecules cross the placenta by several different paths depending on their physicochemical properties. First, small and hydrophobic molecules passively diffuse across the lipid membranes of the placental cells

* Corresponding author at: Department of Chemical Engineering, Carnegie Mellon University, 5000 Forbes Ave, Pittsburgh, PA 15213, United States of America.
E-mail address: kawhite@cmu.edu (K.A. Whitehead).

https://doi.org/10.1016/j.jconrel.2023.07.029
Received 24 May 2023; Received in revised form 11 July 2023; Accepted 17 July 2023
Available online 31 July 2023
0168-3659/© 2023 The Authors. Published by Elsevier B.V. This is an open access article under the CC BY license (http://creativecommons.org/licenses/by/4.0/).

[8,9]. Many prescribed and over-the-counter drugs fall into this category. In addition to passive diffusion, transcellular transport can also occur *via* active receptor-mediated transport or endocytosis and is the mechanism for nutrients and larger molecules like immunoglobulins [10]. Further, some molecules cross the placental barrier through the paracellular space, which are the gaps between the cells in each layer [11].

Placental transport is studied in numerous models, the gold standard of which is the *ex vivo* human placental perfusion method [12,13]. Unfortunately, this method requires access to human placentas donated immediately after birth as well as specialized equipment and techniques. Thus, it is not feasible for most researchers. A slightly more high-throughput model that also uses human tissue is the *ex vivo* placental explant model. These experiments use dissected human placental tissue to study the uptake of compounds into placental cells but are unable to assess transport across the polarized placental barrier [14,15].

Alternatively, *in vivo* experiments have been conducted in a variety of species, including mice, rats, guinea pigs, and sheep [7,16]. Each *in vivo* model has pros and cons in terms of convenience, cost, and similarity to the human placenta [17]. Finally, there are *in vitro* models derived from both primary and immortalized cells. The most common *in vitro* placental model is the BeWo cell line, derived from choriocarcinoma cells. In particular, the BeWo b30 strain, when cultured on semi-permeable membranes, produces a polarized monolayer that decently recapitulates the barrier function of the placenta, despite not showing the fused, multi-nucleated cells that other BeWo lines produce in culture [18–20]. The use of more complex co-culture, microfluidic, and organoid models is an active area of research [21–23].

In this study, we use both the *in vitro* BeWo b30 model and CD-1 mice to establish a fundamental understanding of molecular uptake and transport in the placenta as a function of physicochemical properties. Specifically, we evaluate the effect of molecular weight, conformation, and chemistry on interactions with the placenta. Our findings illustrate that, to obtain a complete picture of placental interactions, uptake into placental cells and transport across the placental layers must be simultaneously considered. Together, these data provide fundamental molecular guidance on the design of medications for safe use during pregnancy.

2. Materials and methods

2.1. Materials

Dulbecco's Modified Eagle Medium Nutrient Mixture F-12/Ham (DMEM-F12), Phosphate buffered saline (PBS), glucose solution, HEPES, Red blood cell lysis buffer, and 5/6-carboxyfluorescein succinimidyl ester (NHS-ester fluorescein) were purchased from ThermoFisher (Waltham, MA). Fetal bovine serum (FBS), Penicillin-Streptomycin, Trypsin-EDTA, Hanks' Balanced Salt Solution (HBSS) were sourced from VWR (Radnor, PA). Collagen from human placental tissue, were obtained from Sigma Aldrich (St. Louis, MO). Flow Cytometry Fixation Buffer was purchased from R&D Systems (Minneapolis, MN). Linear methoxy-polyethylene glycols in 2, 5, 10, 20, and 40 kDa, 4-arm NH_2-modified branched PEGs in 5, 10, and 20 kDa, Diethylaminoethyl-dextran in 20 and 40 kDa, and Carboxymethyl-dextran in 4, 10, and 40 kDa were procured from Creative PEGWorks (Durham, NC). Tomato Lectin-DyLight649™ was purchased from Vector Laboratories (Newark, CA).

2.2. Fluorescent labeling

Branched PEGs with four arms and terminal primary amines were labeled using NHS-ester fluorescein. PEGs were dissolved in deionized H_2O at 10 mg/mL, and NHS-ester fluorescein was dissolved in DMSO at 100 mg/mL. The fluorescein and PEG solutions were combined at a molar ratio of 1:2 NHS-ester fluorescein: amine. Assuming 100% conjugation efficiency, this would result in two fluorescein molecules per PEG molecule. Reactions were stirred at 4 °C overnight. Samples were dialyzed for 72 h against deionized H_2O using Slide-A-Lyzer (ThermoFisher) dialysis cassettes with a 3.5 kDa molecular weight cut off. Samples were then lyophilized and stored at −20 °C until use.

2.3. Cell culture

BeWo b30 cells were gifted from the laboratory of Allen Schwartz (Washington University in St. Louis) and cultured as described by Bode, et al. [19] Specifically, cells were grown in DMEM/F12 medium (Gibco™) supplemented with 10% FBS and 1% penicillin-streptomycin and incubated at 37 °C with 5% CO_2. The cells were passaged using 0.25% trypsin-EDTA solution and used for experiments between passage numbers 30–45. For transport assays, 6.5 mm-diameter Costar® Transwell® membrane supports (Corning, NY) were coated with human placental collagen (130 μg collagen/mm^2 membrane area). Collagen was dissolved in a solution of 20 mM acetic acid and ethanol and applied to the Transwells for 2 h, after which the wells were rinsed with PBS and allowed to dry for 2 h [19]. BeWo b30 cells were seeded at a density of 20,000 cells/well in DMEM-F12 supplemented as described above. BeWo b30 monolayers were grown for 5 days with medium changes every other day. For uptake experiments, cells were seeded in clear 24-well plates at a seeding density of 100,000 cells/well in F12 medium supplemented with 10% FBS and 1% penicillin-streptomycin. Cells were incubated for 48 h before the uptake assays began.

2.4. In vitro transport assays

Before starting transport assays using BeWo b30 monolayers, their transepithelial electrical resistance (TEER) was measured with a Millicell voltohmmeter. Only monolayers with TEER values of 50–100 Ω·cm^2 were used for experiments. The seeding medium was removed, and transport buffer (HBSS with 12.5 mM glucose and 25 mM HEPES) was added to the monolayers and allowed to equilibrate for 1 h at 37 °C. Fluorescently-labeled polymers were dissolved in transport buffer at 0.1 mg/mL for all samples except for sodium fluorescein, which was used at 0.083 mg/mL. The polymer solutions were added to the apical side of the Transwells and incubated on a temperature-controlled shaker (Innova® 40, New Brunswick Scientific) at 37 °C. Samples were collected from the basolateral compartment immediately after adding the polymer solutions, as well as 30, 60, 90, and 120 min later. After sampling, 100 μL of fresh transport buffer was added to the basolateral well to maintain sink conditions. The fluorescence of each sample was measured using a BioTek Synergy2 plate reader at 490/520 nm. Individual calibration curves were made for each polymer sample, then used to convert the fluorescence measurements into the mass of polymer in the basolateral well. The mass of polymer in the basolateral well (Q) was plotted *versus* time (t), and the slope of this line was used to calculate the apparent permeability according to the following equation:

$$P_{app} = \frac{dQ}{dt} \times \frac{1}{A \times C_0} \quad (1)$$

in which dQ/dt is the slope of the line (rate of transport), A is the surface area of the membrane (0.33 mm^2), and C_0 is the apical concentration of polymer. Transport experiments were performed with a minimum of two biological replicates (monolayers seeded from BeWo b30 cells with different passage numbers) and triplicate technical replicates within each experiment.

2.5. In vitro uptake assays

Fluorescent polymer samples were dissolved in transport buffer at the concentrations described above, and these solutions were added to BeWo b30 cells cultured in 24-well plates, as described above. The cells

were incubated with the samples for 2 h before rinsing three times with PBS to remove free fluorescein or polymer molecules. The cells were collected using 0.25% trypsin-EDTA and centrifuged at 2000 ×*g* for five minutes. The cell pellet was resuspended in Flow Cytometry Fixation Buffer and kept on ice for 20 min. Cells were resuspended in PBS with 10% FBS and analyzed using a NovoCyte 3000 (ACEA Biosciences). Data was analyzed using NovoExpress.

2.6. Animal care and use

Animal protocols were approved by the Institutional Care and Use Committee at Carnegie Mellon University (Pittsburgh, PA), and all experiments were performed in accordance with protocol 201,900,014 as well as all institutional, local, and federal regulations. Female CD-1 mice were purchased from Charles River Laboratories. Mice were confirmed pregnant before shipping and arrived on day E15 of pregnancy. Mice were housed individually in standard cages with a 12-h light/dark cycle and free access to water and food.

2.7. In vivo placenta permeability experiments

In vivo experiments were conducted on day E17 of pregnancy in CD-1 mice. Mice received injections of 300 μL of polymer or fluorescent marker solutions intravenously *via* the tail vein. Control mice received phosphate buffered saline (PBS), and treated mice received fluorescein (10 mg/mL) or fluorescently-labeled dextrans or PEG (50 mg/mL). Blood samples were taken from the submandibular vein at $t = 5$, 30, 60, 90, and 120 min after injection. 10 min before the final timepoint, mice were IV injected with 100 μL of 1 mg/mL DyLight649™-conjugated Tomato Lectin to visualize maternal blood vessels. Mice were anesthetized using vaporized isoflurane and live-imaged using a Perkin Elmer *In Vivo* Imaging System IVIS and setting for green fluorescent protein (excitation: 490 nm, emission: 520 nm).

Mice were then sacrificed, and the uterus, liver, spleen, heart, lungs, pancreas, and kidneys were removed from the animal. The liver, spleen, heart, lungs, pancreas, and kidneys were imaged using IVIS at 490/520 nm. The uterus was further dissected to separate each yolk sac and placenta. Fetuses were removed from the yolk sac, and blood was collected *via* cardiac puncture from several fetuses and pooled for analysis due to small collection volumes. Three fetuses and placentas from each mouse were imaged using IVIS. Three placentas from each mouse were transferred to ice-cold DMEM prior to digestion and flow cytometry analysis. The rest of the placentas and fetuses were transferred to 4% formaldehyde for fixation and microscopy.

2.8. Placenta digestion and flow cytometry

The decidua was dissected away from the placentas, which were then washed in ice-cold PBS and cut into small fragments. The fragments were transferred to 1.5 mL digestion medium (DMEM with 500 U/mL Collagenase Type I and 2 U/mL DNAse I) and passed through an 18G syringe needle several times to further dissociate cells. The digestion mixture was incubated for 35 min at 37 °C with 1000 RPM shaking using a VWR Shake-Touch block heater. After this incubation period, the mixture was filtered through a 70 μm cell strainer (VWR) and rinsed with an equivalent volume of cold PBS with 10% FBS. The tissue samples were centrifuged at 5000 ×*g* for 5 min at 4 °C, and the supernatant was removed. Then the sample was incubated with red blood cell lysis buffer at room temperature for 5 min. The sample was centrifuged as above, and the supernatant was discarded. The cells were then washed with 10% FBS in PBS a final time. The cells were divided into equal samples for fixation and staining. Briefly, cells were incubated with LIVE/DEAD™ Fixable Yellow Dead Cell Staining Kit according to manufacturer's instructions (ThermoFisher). Cells were then fixed using Flow Cytometry Fixation Buffer for 20 min on ice. Cells were resuspended in 10% FBS in PBS and analyzed using a NovoCyte 3000 (ACEA Biosciences). Data was analyzed using NovoExpress.

2.9. Histology and microscopy

Tissues were fixed in 4% formaldehyde for 48 h, rinsed extensively with cold PBS, transferred to 30% sucrose, and stored at 4 °C. Tissues were embedded in Sakura Tissue-Tek Optimal Cutting Temperature Compound (OTC; VWR) and stored at −80 °C. Samples were sectioned to 9 μm on a Shandon Cryotome® (Thermo Fisher) and stained with either hematoxylin and eosin for brightfield microscopy or with DAPI for fluorescence microscopy. Imaging was performed using a Keyence BZ-X800 series microscope.

2.10. Statistics

GraphPad Prism (Version 9) was used for all statistical analysis. Significance was assessed by two-tailed Student's *t*-tests or one-way ANOVA where specified. For *in vitro* experiments, at least three biological replicates were performed with three technical replicates each. For *in vivo* experiments, $n = 3$–4 pregnant mice per treatment group, with three placentas used for each flow cytometry experiment and 2–4 fetal blood samples pooled to achieve large enough serum volumes for analysis.

3. Results

There is an urgent need for therapeutics that effectively treat pregnant people while preventing fetal exposure. This study takes the most important first steps towards this aim by improving our understanding of transplacental transport of model drug molecules with varied physiochemical properties. To accomplish this, we examined two biocompatible polymers: dextran, which are branched anhydroglucose molecules, and both linear and branched PEG compounds (Fig. 1). Both polymers are widely studied and commercially available, thus facilitating systemic assessment of permeability over a range of sizes and conformations [24–26].

For both dextran and PEG, their behavior in solution depends on their size. Dextrans below 10 kDa will behave like expandable coils in solution, whereas dextrans above 10 kDa will behave as if they were highly branched [27,28]. In contrast, the linear PEGs are more rod-like at low molecular weights and more coil-like at higher molecular weights [29]. All compounds were fluorescently-labeled with non-degradable linker chemistry to ease measurements. Here, we used FITC-labeled dextrans (FD#) that were 4, 10, 20, 40, and 70 kDa in molecular weight and fluorescein-labeled polyethylene glycols (PEG#) in weights of 2, 5, 10, 20, and 40 kDa. We also compared the transport of these macromolecules to the small molecule, sodium fluorescein (FL, 376 Da), which is the same fluorophore present in the labeled polymers. To probe the influence of molecular conformation, we included linear and 4-arm branched PEG compounds. The molecular weights of these compounds were analogous to those listed above.

3.1. Transplacental permeability in vitro depends on size, structure, and chemistry

First, we examined the permeability of our model compounds across BeWo b30 placental cell monolayers in Transwells. For these experiments, the fluorescently-labeled polymers were incubated in the apical ("maternal") compartment, and samples of medium were collected from the basolateral ("fetal") well over a period of two hours. Apparent permeability (P_{app}) was calculated using Eq. (1) and is shown in Fig. 2. As expected, permeability decreased with molecular weight for both dextrans and PEGs with a significant linear relationship assessed by a one-way ANOVA.

For similar sizes, the PEGs crossed the placental barrier at roughly twice the rate of the dextrans. This suggests that chemical and/or

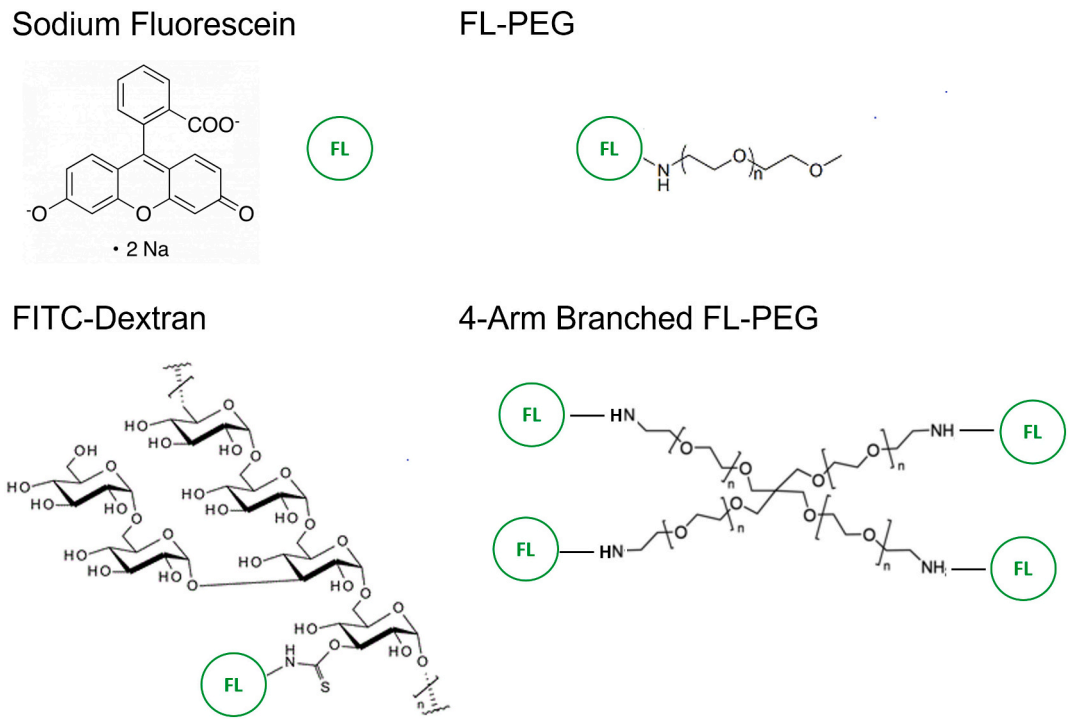

Fig. 1. Chemical structures of dextran and PEG derivatives.

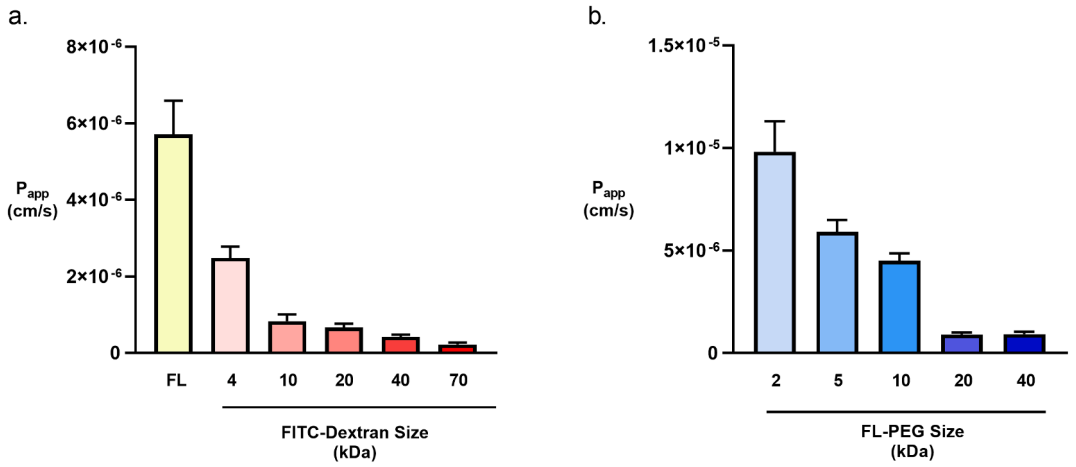

Fig. 2. Macromolecular permeability across BeWo placental monolayers is size-dependent. (A) Sodium fluorescein (FL), FITC-dextrans, and (B) linear FL-PEGs of varied molecular weights were applied to BeWo b30 monolayers, and the apparent permeability (P_{app}) was measured over two hours. For both dextrans and PEGs, P_{app} inversely correlated with molecular weight, with a significant linear trend determined by one-way ANOVA ($p < 0.0001$). Error bars represent SEM, $n = 2$–4 biological replicates with 3 technical replicates each.

conformational differences also influence permeability, although not to the same degree as molecular weight for these specific polymers. To probe the importance of molecular shape, we next examined the permeability of fluorescein-labeled 4-arm PEGs with weights of 5, 10, and 20 kDa (See Fig. 3).

For 5 and 10 kDa PEG, the 4-arm branched versions had lower permeability than their linear counterparts. For the 20 kDa PEG, there was no significant difference between the permeability of the two conformations. It is possible that branching makes the structures more rigid, while the linear molecule can adopt a very compact structure that more easily permeates the cell barrier. The 4-arm PEGs were compared to dextrans of the same molecular weight. At 5 kDa, the PEG and dextran had similar, high apparent permeability. At larger molecular weights, the dextrans were significantly less permeable than the branched PEG, suggesting that chemistry is an important factor in placental transport.

3.2. Polymer chemistry influences placental uptake in vitro more than size

In addition to translocation across BeWo b30 monolayers, we were interested in molecular uptake into BeWo cells, as these are independent transport phenomena. For these experiments, fluorescein, dextran, or PEG treatments were incubated for 2 h with BeWo b30 cells that had not been differentiated into monolayers. Then, the cells were analyzed by flow cytometry for fluorescein signal. All compounds accumulated in 10–35% of placental cells, with no significant differences between groups (Fig. 4).

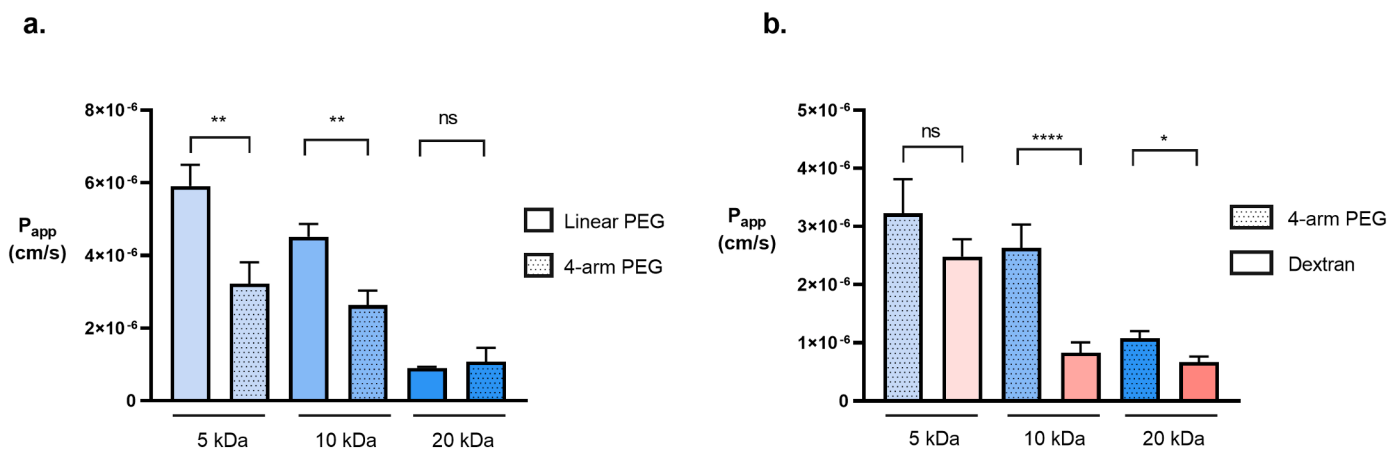

Fig. 3. Branching and chemistry affect permeability in BeWo b30 monolayers. FITC-dextrans and fluorescein-labeled PEG molecules with linear or 4-arm structures were applied to BeWo b30 placental monolayers, and apparent permeability was measured over two hours. (A) The permeability of lower molecular weight PEG samples was affected by conformation. (B) Comparing branched PEGs and dextrans of equivalent sizes shows that chemistry also affects transport for molecules with similar conformation. Error bars represent SEM. $n = 3$ biological replicates with 3 technical replicates each. $^*p < 0.05$, by two-tailed Student's *t*-test.

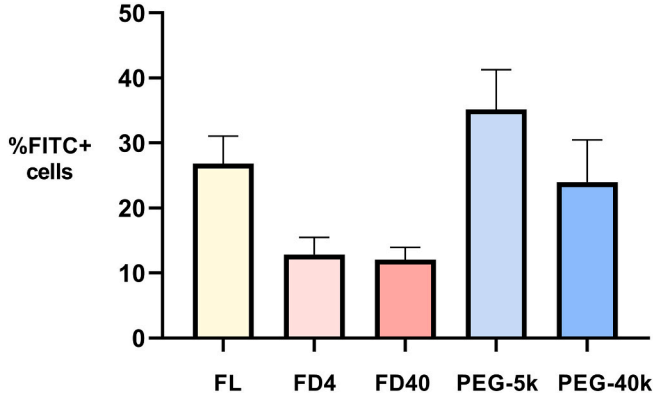

Fig. 4. Placental BeWo cells take up marker molecules independently of size and chemistry. (A) Sodium fluorescein (FL) and fluorescently labeled dextrans (FD4 and FD40) and linear PEGs were incubated with BeWo cells for 2 h *in vitro*, and uptake was assessed by flow cytometry. All groups had average values of at least 10% FITC+ cells, and no significant differences existed between groups. Error bars represent SEM, $n = 2$, with four technical replicates each.

3.3. Size and chemistry affect transplacental transport in pregnant mice

Next, we asked whether the transport and uptake trends observed in human placental cell culture held in a mouse model. For these experiments, pregnant CD-1 mice on day 17 of pregnancy were intravenously injected with fluorescein (100 mg/kg), FD4, FD40, PEG-5 k, or PEG-40 k (all 500 mg/kg). Post-injection, blood samples were collected over a period of two hours, at which point the dams were live imaged using IVIS and then euthanized for imaging of the intact amniotic sacs, placentas, and fetuses. Each dam was gestating between 12 and 16 fetuses. Because fetal blood volumes were low, blood was pooled from 2 to 4 fetuses for fluorometric quantification. Three of the placentas were digested and prepared as a single cell suspension for analysis using flow cytometry, and intact amniotic sacs, placentas, and fetuses were fixed in formaldehyde for histology.

Maternal blood concentrations peaked immediately after injection for all treatment groups and decreased at different rates over two hours (Fig. 5a). Interestingly, molecular partitioning across the placental barrier varied dramatically with size, as is evident when comparing the fetal and maternal blood concentrations from the final timepoint (Fig. 5b). Specifically, after two hours, the concentrations of the small molecule fluorescein in the maternal and fetal blood were nearly identical, indicating free diffusion across the placental barrier. FD4 also readily crossed the placenta, with no significant difference between the fetal and maternal blood concentrations. For FD40, PEG-5 k, and PEG-40 k, the fetal concentrations were significantly lower than those in the dam. The low concentration of polymer in the fetal blood suggests that the placenta prevents the transport of these macromolecules. The difference in partitioning of the similarly-sized FD4 and PEG5 suggests that structure and/or chemistry is playing a role in the transport mechanism. It is possible that different conformations are affecting paracellular transport, while the chemistry may impact uptake and retention in the placental cells.

To further investigate the barrier function of the placenta, we used IVIS imaging to assess the distribution between the placenta and the fetus. In these experiments, three fetuses and placentas and one intact amniotic sac from each dam were imaged, and total fluorescent flux was measured. In the assessment of these images, it is critical to note that these placentas were freshly excised and had not been cleared of blood. Because the placenta is so highly vascularized, IVIS will capture fluorescence from cells with internalized marker molecules as well as from the blood within the vessels. For fluorescein, there was no significant difference between the two values, as both fetus and placenta were highly fluorescent (Fig. 5c). For FD40, PEG5, and PEG40, the fetus had much less fluorescence than the placenta, and for the largest polymers, FD40 and PEG40, there was almost no measurable fluorescence in the fetus. The size dependence of macromolecular transport across the placenta is illustrated by comparing the ratios of the fetal flux to the placental flux, which are significant when comparing FD4 to FD40 and PEG5 to PEG40 (Fig. 5d). Representative images are shown in Fig. 5e-f.

Based on the maternal serum profiles (Fig. 5a), fluorescein and FD4 concentrations decreased more rapidly than the larger polymers, although both remained well above the limit of detection at 2 h. To assess the shorter-term kinetics of placental transport for these rapidly clearing molecules, pregnant mice were injected with fluorescein or FD4 at the same concentrations as the previous experiments. The mice were sacrificed 30 min after injection, and blood and tissue samples were processed as above. For the fluorescein-treated mice, the fetal concentration is lower than the maternal concentration at 30 min, but it is less than an order of magnitude different. For the FD4-treated mice, the fetal concentration at 30 min is nearly two orders of magnitude lower than the maternal concentration, and this difference disappears by two hours. (Fig. 6a) This slower diffusion rate across the placenta suggests that transport is more restricted for FD4 as compared to the smaller FL.

When comparing IVIS images from 30 min and 2 h after injection, there is no significant difference between the ratio of fetal-placental flux

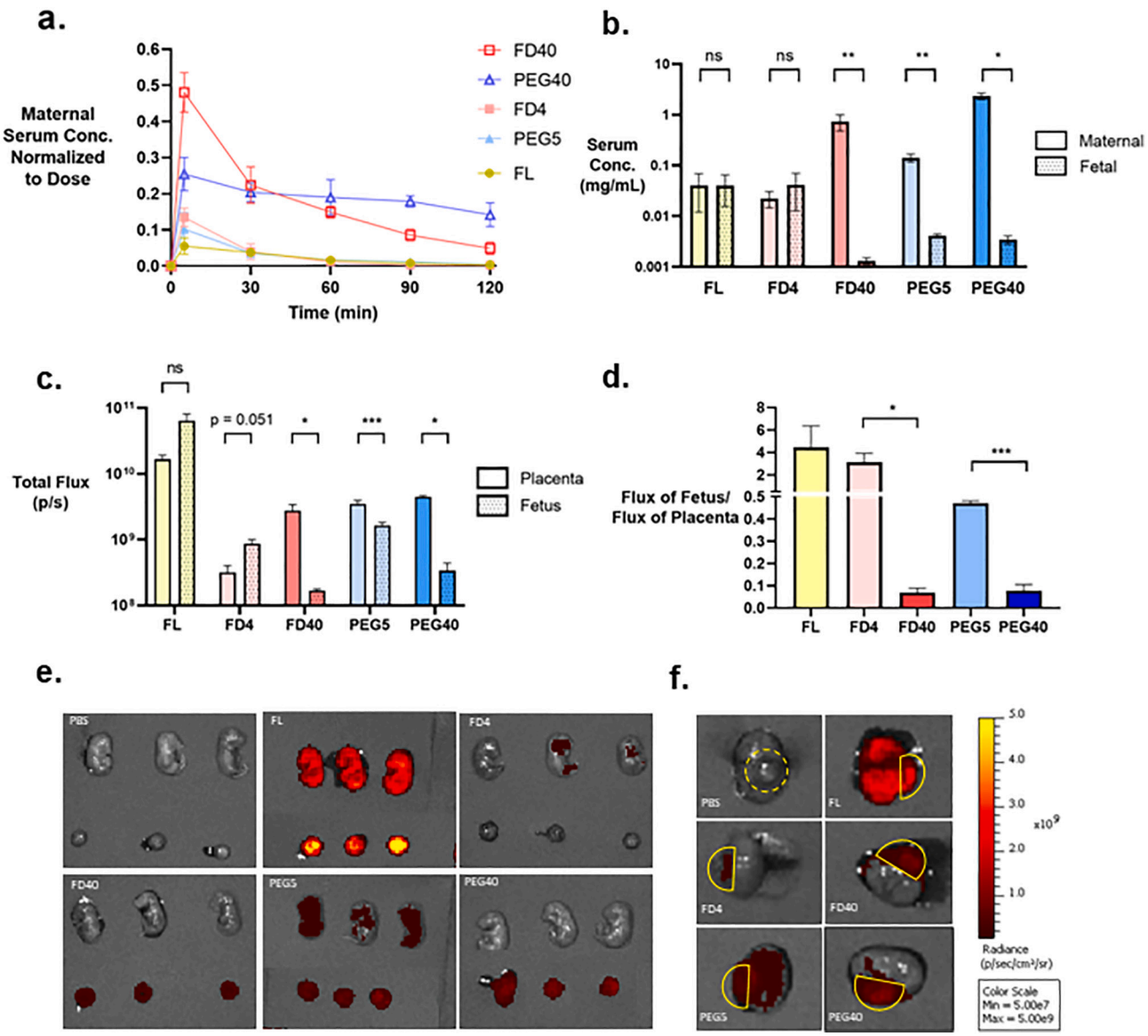

Fig. 5. Molecular weight and polymer chemistry affect pharmacokinetics and transplacental transport in pregnant mice. (A) Pregnant CD-1 mice were injected with fluorescein, FD4, FD40, PEG5, or PEG40, and blood samples were collected over two hours. (B) Only FD40, PEG5, and PEG40 resulted in maternal and fetal blood concentrations that were significantly different. Error bars represent SEM. Statistical significance was assessed by ratio paired two-tailed Student's *t*-test. $n = 3$. The fluorescence of placentas and fetuses was quantified by IVIS imaging. (C) For FD40, PEG5, PEG40, the placentas had higher fluorescence signal than the fetuses. Statistical significance was assessed by ratio paired, two-tailed Student's t-test. n = 3. (D) The ratio of fetal flux to placental flux shows that partitioning between the fetus and placenta is dependent on molecular weight. Significance assessed by unpaired, two-tailed Student's t-test. n = 3. Error bars represent SEM. $^{*}p < 0.05$, $^{***}p < 0.005$. (E) Representative IVIS images of fetuses and placentas taken at 2 h after injection. (F) Representative images of amniotic sacs with placentas outlined in yellow. For the PBS mouse, the dashed yellow line indicates a placenta located on top of the amniotic sac, rather than in profile as in the rest of the images. Only fluorescein and PEG5 visibly accumulated in the fetus. (For interpretation of the references to colour in this figure legend, the reader is referred to the web version of this article.)

for fluorescein. (Fig. 6b) For FD4, this ratio goes from <1 after 30 min to >1 after 2 h. (Fig. 6c) This means that after 30 min, the FD4 is still mostly concentrated in the maternal blood flowing through the placenta. After 2 h however, the fluorescence is higher in the fetus, suggesting that the FD4 has diffused or been actively transported into the fetal blood system, while it has largely cleared from the maternal blood. This is reflected in the representative IVIS images shown in Fig. 6d-e.

3.4. Size and chemistry affect uptake by placental cells in vivo

While our data show that the physicochemical properties of drugs affect their distribution between the fetal and maternal compartments, it is not clear how these properties affect placental cell uptake and retention *in vivo*. To assess polymer uptake by placental cells, the placentas from treated mice were analyzed using flow cytometry (Fig. 7a). For the small molecule fluorescein, despite the nearly equal concentrations of fluorescein in the fetal and maternal blood, very little was present inside placental cells (<1% FITC+ cells). For dextran molecules, FD40 accumulated to a greater degree in placental cells (48% FITC+ cells) compared to FD4 (5% FITC+ cells). In contrast, the placentas in PEG-treated mice had nearly equivalent percentages of FITC+ cells regardless of PEG size (54% for PEG-5 k and 52% for PEG-40 k). The chemical difference between dextran and PEG appears to affect uptake by placental cells only for the smaller molecular weight. The percentage of FITC+ cells is significantly higher for the placentas from mice

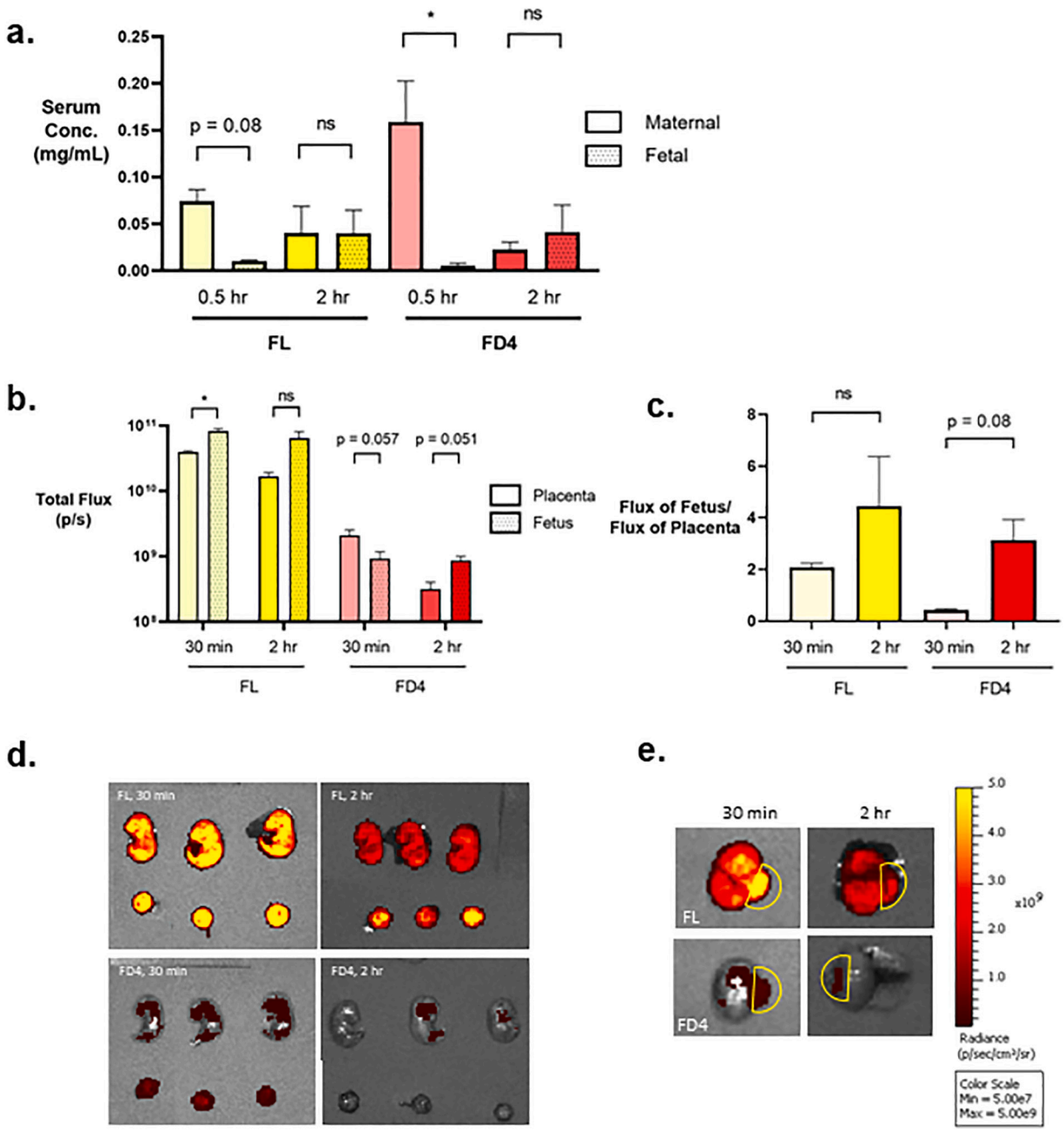

Fig. 6. Partitioning of FL and FD4 between the placenta and fetus changes over time. Pregnant mice were injected with fluorescein or FD4, and serum concentrations and fluorescence distribution were assessed 30 min and 2 h after injection. (A) The concentration differences over time shows that FL transport across the placenta is more rapid than that of FD4. (B) IVIS imaging shows that FD4 distribution between placenta and fetus changes between 30 min and 2 h after injection. Statistical significance assessed by ratio-paired, two-tailed Student's *t*-test. $n = 2$. (C) Replotting the flux data as a ratio of fetal flux to placental flux shows that FD4 is more concentrated in the placenta after 30 min (ratio < 1) but higher in the fetus after two hours (ratio > 1). Statistical significance assessed by unpaired, two-tailed Student's t-test. n = 2. Error bars represent SEM. $^*p < 0.05$ (D) Representative IVIS images of fetuses and placentas taken at 30 min and 2 h after injection. Each set of 3 fetuses and placentas are from the same dam. (E) Representative IVIS images of intact amniotic sacs taken 30 min and 2 h after injection.

receiving PEG5 as compared to FD4 ($p < 0.01$ by unpaired, two-tailed Student's *t*-test, $n = 3$). However, this difference is not seen for the 40 kDa polymers, both of which are taken up by around 50% of cells.

We were curious as to whether the time dynamics observed in serum measurements and IVIS images for fluorescein and FD4 would extend to cellular uptake. The diffusion of fluorescein into the cells of the placenta is minimal, but it reaches its final concentration rapidly, as the percentage of FITC+ cells at 30 min and 2 h is nearly identical. In contrast, FD4 has entered only about 0.2% of cells after 30 min, but by 2 h, it is in approximately 1.25% of cells. (Fig. 7b) This is likely due to the larger size of FD4 decreasing the rate of simple diffusion across cell membranes and may also be affected by differences in active transport mechanisms for the two compounds.

Fluorescence microscopy visually confirmed our quantitative measurements of the distribution of different fluorescent compounds throughout the placental tissue. In these experiments, intact amniotic sacs and dissected placentas were prepared for histology. Sections were stained with hematoxylin and eosin (H&E) to aid in identifying regions of the placenta (Fig. 8a-b). Once the placental regions were identified, we next used fluorescence microscopy to visualize the distribution of the model drugs (Fig. 8c). By E17, fetal red blood cells are mature and do not contain nuclei as they do earlier in development. Thus, to identify

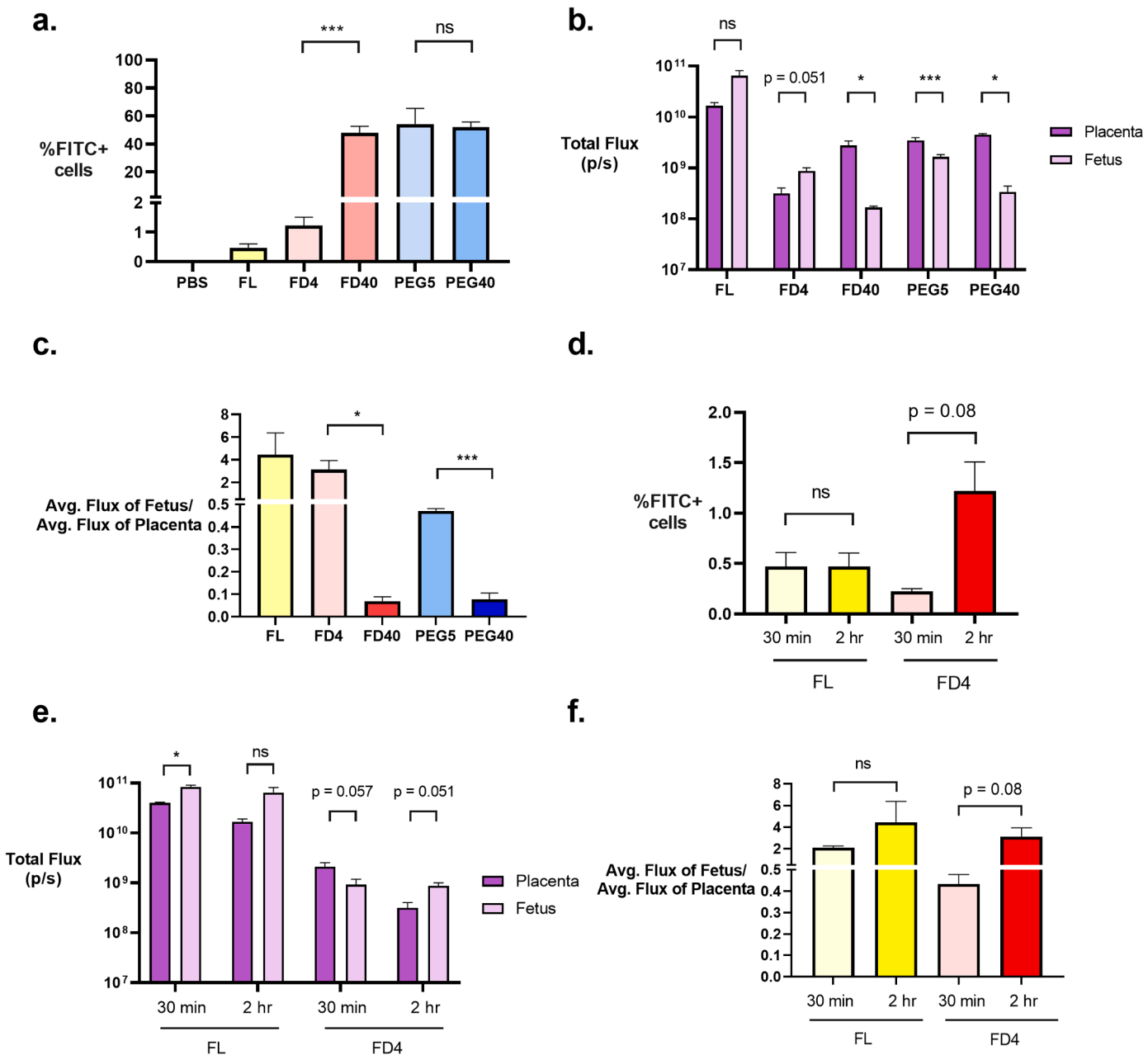

Fig. 7. Molecular weight affects polymer uptake by placental cells *in vivo*. CD-1 mice on day 17 of pregnancy were injected with fluorescein, FD4, FD40, PEG5, or PEG40. After 30 min or two hours, mice were sacrificed, and placentas were dissected and processed for flow cytometry. (A) Uptake of fluorescent compounds into placental cells varied by molecular weight, with the small molecule fluorescein accumulating in <1% FITC+ cells and larger compounds entering up to 55% of cells. (B) The percentage of placental cells containing fluorescein is the same at both timepoints, but for FD4, the percentage of FITC+ cells increases over time. Significance determined by unpaired, two-tailed Student's *t*-test. Error bars represent SEM. ***$p < 0.005$. $n = 3$.

maternal and fetal blood vessels, we IV-injected the pregnant mice with DyLight649™-conjugated Tomato Lectin 10 min before they were euthanized. Tomato lectin binds to specific carbohydrate molecules located on the surface of endothelial cells, and therefore is widely used to visualize blood vessels [30]. Because lectin is large (~71 kDa), it remains in the maternal bloodstream and can be seen surrounding maternal vessels but not elsewhere in the placental sections.

As seen in Fig. 8c panel (ii), there is no visible signal in the FITC channel, confirming our observation that the small molecule fluorescein is not retained in placental cells. In contrast, FITC-signal is visible in cells throughout the labyrinth region (L) in panels iii-vi, which show placentas from mice treated with FD4, FD40, PEG5, and PEG40. The labyrinth is the part of the placenta where the fetal and maternal vessels intermingle, and transport occurs across the layers of syncytiotrophoblasts and trophoblast layers [31,32]. The small fetal vessels come together and form larger vessels in the chorionic plate (CP) and ultimately form the umbilical cord. Importantly, while FITC signal is visible in the labyrinth and areas surrounding the maternal vessels (MV), it is not seen around the fetal vessels (FV) or the chorionic plate. This confirms our observations that while dextrans and PEG are retained in placental cells, they do not enter the fetal blood system.

4. Discussion

Perinatal health is a critically under-researched area, and the consequences are severe, with a mortality rate of about 24 maternal deaths

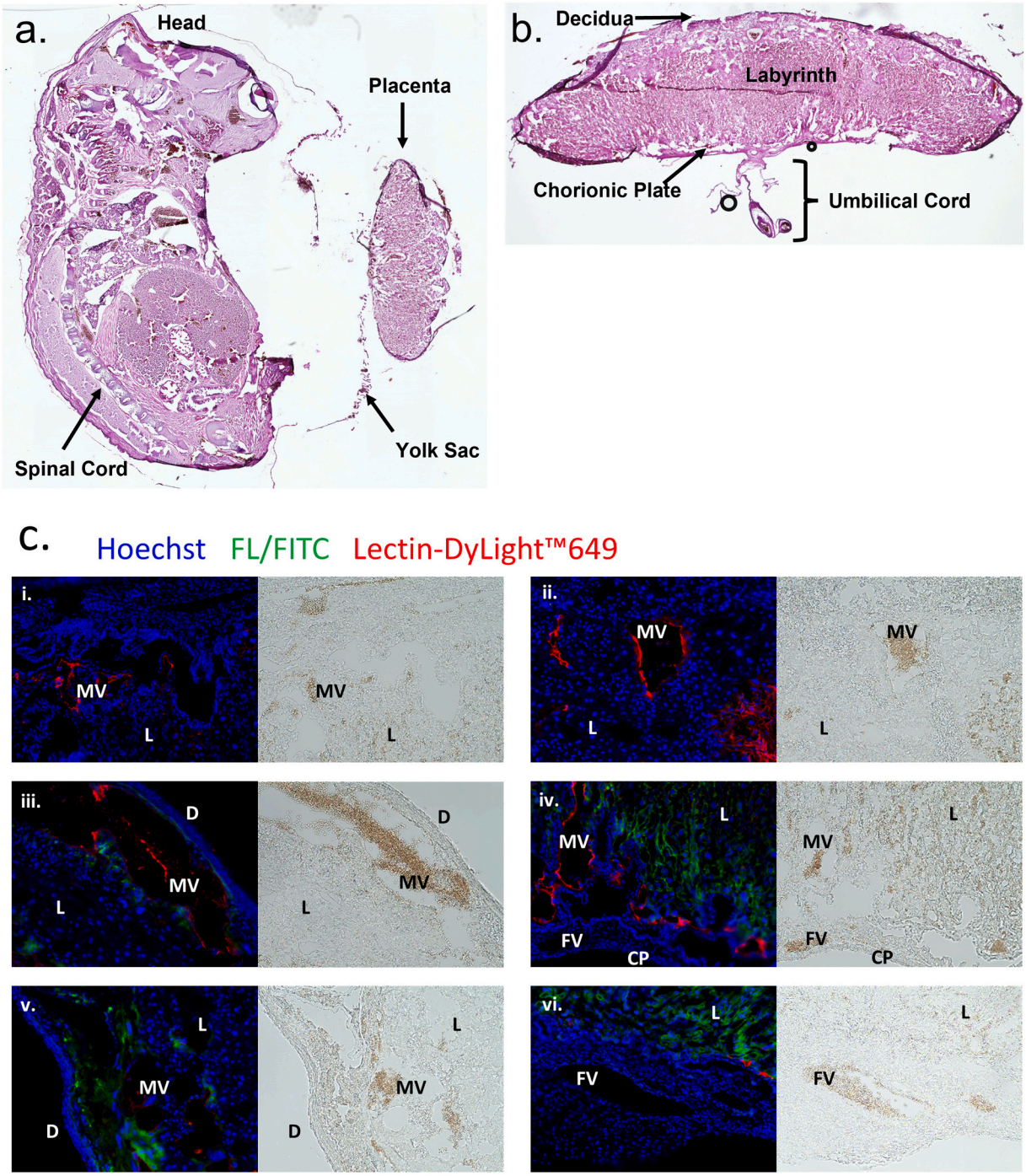

Fig. 8. Molecular properties determine distribution in placental tissue. E17 amniotic sacs were dissected and processed for histology intact or further dissected for isolated placenta imaging. (A) Cross section of an E17 fetus in an intact amniotic sac, stained with hematoxylin and eosin (H&E) to show the placenta in its original orientation with the yolk sac still partially intact. (B) H&*E*-stained cross section of the E17 placenta showing the regions of interest: decidua (D), labyrinth (L), chorionic plate (CP), and umbilical cord. (C) Fluorescent images of placenta cross sections from pregnant mice injected with (i) PBS (control), (ii) FL, (iii) FD4, (iv) FD40, (v) PEG5, and (vi) PEG40. Tissue was stained with Hoechst to visualize nuclei, and the fluorescently-labeled molecules appear in green. Mice were IV injected with DyLight 649™-conjugated lectin 10 min before they were euthanized to differentiate maternal blood vessels (MV) from fetal blood vessels (FV). In (ii), no signal from FL is present, confirming that it is not retained in placental cells. In iii-vi, varying levels of FITC signal are visible in the labyrinth but not in the immediate surroundings of the fetal vessels or the chorionic plate where the fetal vasculature coalesces into the umbilical cord. (For interpretation of the references to colour in this figure legend, the reader is referred to the web version of this article.)

per 100,000 live births in the United States (CDC, 2020). Our lack of pharmacological knowledge during pregnancy means that many pregnant people are undermedicated because of real or perceived risk to the fetus [2,33,34]. In a small number of recent reports, polymers have been conjugated to small molecule drugs to change their interactions with the placenta and prevent fetal drug exposure [6,15]. The number of materials that have been assessed as drug carriers for this purpose is very small; thus, we designed this study of the transport of the biocompatible polymers dextran and PEG across the placenta to better understand which molecular properties of nanomaterials affect their interaction

with the placenta.

In this work, we used sodium fluorescein (MW 376 Da) as our model small molecule drug that freely crosses the placenta. To model drug-polymer conjugates, we used dextrans and PEGs labeled with fluorescein isothiocyanate in different molecular weights and structures. They were studied in an *in vitro* model of the placenta, the BeWo b30 cell line, as well as in pregnant CD-1 mice. In both models, transport was size dependent. As expected, the small molecule fluorescein was highly permeable because its small molecular weight enables diffusion across the cell membrane as well as passage through tight junctions. In BeWo b30 monolayers, dextrans and PEGs up to 10 kDa permeated the barrier. In mice, a similar dependence on size was observed. While FD4 crossed the placenta and reached moderate concentrations in the fetus, FD40 was almost entirely excluded. *In vivo*, PEG5 crossed the placenta less than FD4, which was unexpected based on the *in vitro* data. This could be attributed to the many differences between BeWo b30 cells and the placenta, as it has been reported that BeWo b30 cells are inherently less permeable than placental tissue based on TEER and nanoparticle transport experiments [35]. In mice, both FD40 and PEG40 experienced negligible trans-placental transport as expected based on the *in vitro* experiments.

Although the identification of *in vitro-in vivo* correlations would be of marked utility in drug development, the predictivity we observed for the permeability assays in BeWo b30 cells did not hold up for cellular uptake. Regarding uptake, BeWo cells took up all model drug compounds to a similar extent; however, dramatic differences in drug accumulation were observed for placenta cells in mice. While few placental cells took up fluorescein and FD4, ~40% of cells contained FD40, PEG5, and PEG40. This disconnect between *in vitro* and *in vivo* results is not surprising, given the biological and physical differences between cell culture configurations and a functioning placenta [18]. For example, the *in vitro* uptake experiments were performed under static conditions with no mechanism of clearance. Therefore, it is unsurprising that fluorescein was present in more cells than *in vivo*, given that culturing conditions presented a constant, high concentration gradient to drive simple diffusion. The *in vitro* uptake of PEG increased as it did *in vivo*, but the dextran uptake, particularly FD40 was much lower. This is likely due to the fact that large dextrans are primarily taken up by micropinocytosis, which BeWo b30 cells do not perform unless stimulated using forskolin [36,37].

As discussed above, *in vitro* models are often inadequate, and because of this, *ex vivo* studies are common in the study of placental transport. The gold standard is the perfusion of a whole human placenta, which produces data that correlate robustly with clinical studies [12,18,38]. Unfortunately, this technique is inconvenient and technically challenging, meaning that few researchers have access, and those that do are limited by throughput. To address these challenges of *ex vivo* placenta studies, the explant model is used, in which small pieces of human placenta are incubated in solutions containing the compounds of interest [39]. This model, however, has another important limitation: while it is useful for placental cell uptake experiments, it cannot assess trans-placental transport, particularly for molecules that undergo paracellular transport. This is because the placental barrier is not polarized as it is *in vivo*, and there is no separation of maternal and fetal compartments. Therefore, the critical question of fetal exposure remains unanswered because cellular uptake does not guarantee transport. This is seen in our data for FD40 and PEG40, which accumulate in nearly 40% of placental cells but cross into the fetal blood negligibly. The explant model was used in a 2022 study by Dodd, et al., in which a small molecule drug was conjugated to 2 kDa and 6 kDa PEG, significantly reducing its uptake into the placental explants [15]. However, the data presented here go beyond uptake alone and suggest that PEG molecules of those sizes would still be able to cross into the fetal blood.

To prevent fetal exposure during pregnancy, polymer-drug conjugates will require a unique array of characteristics. To that end, our data suggest that a larger polymer, perhaps as large as 40 kDa, may be a good choice. However, the 40 kDa dextran and PEG were readily taken up by placental cells. At the time scale of 2 h that we studied, the polymers do not reach the fetal blood compartment or tissue, but it is possible that transfer may occur at longer times. Depending on the polymer size and chemistry, it could be cleared from placental tissue before any significant diffusion or exocytosis into the fetus occurs. The question of biocompatibility and toxicity would be critical in the development of such a drug delivery system. While we chose two polymers widely considered to be non-toxic and confirmed that they did not cause cytotoxicity *in vitro*, the effect of repeat dosing would require evaluation to ensure that the polymers do not build up in the placental cells or fetus over time. Finally, consideration would need to be given to the effect of the polymer or conjugation process on the biological activity of the drug. The use of cleavable or biodegradable polymers such as PLGA or modified PEGs could mitigate these concerns [40,41].

5. Conclusion

It is well known that molecular properties affect drug transport across biological barriers and biodistribution, but these phenomena are not equally studied in all tissues. In particular, there is a lack of understanding surrounding transplacental transport and the safety of drugs during pregnancy. Here, we examined drug transport in an *in vitro* model of the placenta as well as in pregnant mice. We found that two widely-used and biocompatible polymers, dextran and PEG, differed in their transport behavior depending on their molecular weight, conformation, and chemistry. Increasing molecular weight decreased transport across the placental barrier both *in vitro* and *in vivo*; however, the large polymers were readily taken up by placental cells, emphasizing the importance of using models that allow the measurement of both permeability and uptake. These data will inform the future development of pharmaceutical formulations that treat maternal conditions without fetal exposure to potentially harmful drugs.

CRediT authorship contribution statement

Katherine C. Fein: Writing – review & editing, Writing – original draft, Methodology, Investigation, Formal analysis, Data curation, Conceptualization. **Mariah L. Arral:** Writing – review & editing, Methodology, Investigation. **Julie S. Kim:** Writing – review & editing, Investigation. **Alexandra N. Newby:** Writing – review & editing, Methodology, Investigation. **Kathryn A. Whitehead:** Writing – review & editing, Supervision, Project administration, Funding acquisition, Conceptualization.

Declaration of Competing Interest

None.

Data availability

Data will be made available on request.

Acknowledgments

Funding for the project was provided by the National Institutes of Health (NIH) Director's New Innovator Award, grant number DP2-HD098860. M.L.A. was supported by an NSF Graduate Research Fellowship (award number DGE1745016) and by an NIH F31 Fellowship (award number 1F31AG077874-01A1). BeWo b30 cells were generously gifted by Allen Schwartz. Graphical abstract created using Biorender.com.

References

[1] A.A. Mitchell, S.M. Gilboa, M.M. Werler, K.E. Kelley, C. Louik, S. Hernández-Díaz, Medication use during pregnancy, with particular focus on prescription drugs: 1976-2008, Am. J. Obstet. Gynecol. 205 (1) (2011) 51.e1–51.e8, https://doi.org/10.1016/j.ajog.2011.02.029.

[2] A.Z. Bauer, S.H. Swan, D. Kriebel, Z. Liew, H.S. Taylor, C.G. Bornehag, A. M. Andrade, J. Olsen, R.H. Jensen, R.T. Mitchell, N.E. Skakkebaek, B. Jégou, D. M. Kristensen, Paracetamol use during pregnancy — a call for precautionary action, Nat. Rev. Endocrinol. 17 (12) (2021) 757–766, https://doi.org/10.1038/s41574-021-00553-7.

[3] M.M. Lynch, L.B. Squiers, K.M. Kosa, S. Dolina, J.G. Read, C.S. Broussard, M. T. Frey, K.N. Polen, J.N. Lind, S.M. Gilboa, J. Biermann, Making decisions about medication use during pregnancy: implications for communication strategies, Matern. Child Health J. 22 (1) (2018) 92–100, https://doi.org/10.1007/s10995-017-2358-0.

[4] M.R. Syme, J.W. Paxton, J.A. Keelan, Drug transfer and metabolism by the human placenta, Clin. Pharmacokinet. 43 (8) (2004) 487–514, https://doi.org/10.2165/00003088-200443080-00001.

[5] A. Sharma, N. Sah, S. Kannan, R.M. Kannan, Targeted drug delivery for maternal and perinatal health: challenges and opportunities, Adv. Drug Deliv. Rev. 177 (2021), 113950, https://doi.org/10.1016/j.addr.2021.113950.

[6] A.R. Menjoge, R.S. Navath, A. Asad, S. Kannan, C.J. Kim, R. Romero, R.M. Kannan, Transport and biodistribution of dendrimers across human fetal membranes: implications for intravaginal Administration of Dendrimer-Drug Conjugates, Biomaterials 31 (18) (2010) 5007–5021, https://doi.org/10.1016/j.biomaterials.2010.02.075.

[7] M.R. Dilworth, C.P. Sibley, Review: transport across the placenta of mice and women, Placenta 34 (SUPPL) (2013) S34–S39, https://doi.org/10.1016/j.placenta.2012.10.011.

[8] W. Lell, K. Liber, F. Snyder, A quantitative study of placental transmission and the permeability of fetal membranes at various stages of pregnancy, Am. J. Phys. 100 (1) (1931) 21–31.

[9] B.L. Mirkin, Diphenylhydantoin: placental transport, fetal localization, neonatal metabolism, and possible teratogenic effects, Obstet. Gynecol. Surv. 26 (9) (1971) 645–646, https://doi.org/10.1097/00006254-197109000-00012.

[10] H. Schneider, R.K. Miller, Receptor-mediated uptake and transport of macromolecules in the human placenta, Int. J. Dev. Biol. 54 (2–3) (2010) 367–375, https://doi.org/10.1387/ijdb.082773hs.

[11] I. Uehara, T. Kimura, S. Tanigaki, T. Fukutomi, K. Sakai, Y. Shinohara, K. Ichida, M. Iwashita, H. Sakurai, Paracellular route is the major urate transport pathway across the blood-placental barrier, Phys. Rep. 2 (5) (2014) 1–10, https://doi.org/10.14814/phy2.12013.

[12] M. De Sousa Mendes, D. Hirt, C. Vinot, E. Valade, G. Lui, C. Pressiat, N. Bouazza, F. Foissac, S. Blanche, M.P. Lê, G. Peytavin, J.M. Treluyer, S. Urien, S. Benaboud, Prediction of human fetal pharmacokinetics using ex vivo human placenta perfusion studies and physiologically based models, Br. J. Clin. Pharmacol. 81 (4) (2016) 646–657, https://doi.org/10.1111/bcp.12815.

[13] M. Knöfler, S. Haider, L. Saleh, J. Pollheimer, T.K.J.B. Gamage, J. James, Human placenta and trophoblast development: key molecular mechanisms and model systems, Cell. Mol. Life Sci. 76 (18) (2019) 3479–3496, https://doi.org/10.1007/s00018-019-03104-6.

[14] K. Alhareth, L. Valero, K.E. Mohamed, L. Fliedel, C. Roques, S. Gil, N. Mignet, T. Fournier, K. Andrieux, Qualitative and quantitative analysis of the uptake of Lipoplexes by villous placenta explants, Int. J. Pharm. 567 (June) (2019), 118479, https://doi.org/10.1016/j.ijpharm.2019.118479.

[15] A. Dodd, A.A. Natfji, A. Evangelinos, A. Grigoletto, G. Pasut, F. Beards, L. Renshall, H.M.I. Osborn, F. Greco, L.K. Harris, Conjugation to PEG as a strategy to limit the uptake of drugs by the placenta: potential applications for drug Administration in Pregnancy, Mol. Pharm. 19 (1) (2022) 345–353, https://doi.org/10.1021/acs.molpharmaceut.1c00498.

[16] J.S. Barry, R.V. Anthony, The pregnant sheep as a model for human pregnancy, Theriogenology 69 (1) (2008) 55–67, https://doi.org/10.1016/j.theriogenology.2007.09.021.

[17] M.S. Mohamed, S. Veeranarayanan, A.C. Poulose, Y. Nagaoka, H. Minegishi, Y. Yoshida, T. Maekawa, D.S. Kumar, Type 1 Ribotoxin-Curcin conjugated biogenic gold nanoparticles for a multimodal therapeutic approach towards brain Cancer, Biochim. Biophys. Acta 1840 (6) (2014) 1657–1669, https://doi.org/10.1016/j.bbagen.2013.12.020.

[18] M.S. Poulsen, E. Rytting, T. Mose, L.E. Knudsen, Modeling placental transport: correlation of in vitro BeWo cell permeability and ex vivo human placental perfusion, Toxicol. in Vitro 23 (7) (2009) 1380–1386, https://doi.org/10.1016/j.tiv.2009.07.028.

[19] C.J. Bode, H. Jin, E. Rytting, P.S. Silverstein, A.M. Young, K.L. Audus, In vitro models for studying trophoblast transcellular transport, Methods Mol. Med. 122 (2006) 225–239, https://doi.org/10.1385/1-59259-989-3:225.

[20] H. Li, B. Van Ravenzwaay, Assessment of an in Vitro Transport Model Using BeWo B30 Cells to Predict Placental Transfer of Compounds, 2013, pp. 1661–1669, https://doi.org/10.1007/s00204-013-1074-9.

[21] M.Y. Turco, L. Gardner, R.G. Kay, R.S. Hamilton, M. Prater, M.S. Hollinshead, A. McWhinnie, L. Esposito, R. Fernando, H. Skelton, F. Reimann, F.M. Gribble, A. Sharkey, S.G.E. Marsh, S. O'rahilly, M. Hemberger, G.J. Burton, A. Moffett, Trophoblast organoids as a model for maternal–fetal interactions during human placentation, Nature 564 (7735) (2018) 263–281, https://doi.org/10.1038/s41586-018-0753-3.

[22] L. Aengenheister, K. Keevend, C. Muoth, R. Schönenberger, L. Diener, P. Wick, T. Buerki-Thurnherr, An advanced human in vitro co-culture model for translocation studies across the placental barrier, Sci. Rep. 8 (1) (2018) 1–12, https://doi.org/10.1038/s41598-018-23410-6.

[23] R.L. Pemathilaka, D.E. Reynolds, N.N. Hashemi, Drug transport across the human placenta: review of placenta-on-a-chip and previous approaches, Interface Focus 9 (5) (2019), https://doi.org/10.1098/rsfs.2019.0031.

[24] Patel, SIGMA Product Information FITC Dextran, 2019.

[25] N. Dextran, Dextran and Dextran derivatives. 11, Acid Hydrolysis. 2 (1964) 35–42.

[26] A. Kolate, D. Baradia, S. Patil, I. Vhora, G. Kore, A. Misra, PEG - a versatile conjugating ligand for drugs and drug delivery systems, J. Control. Release 192 (2014) 67–81, https://doi.org/10.1016/j.jconrel.2014.06.046.

[27] K.A. Granath, Solution properties of branched Dextrans, J. Colloid Sci. 13 (4) (1958) 308–328, https://doi.org/10.1016/0095-8522(58)90041-2.

[28] Sigma, Fluorescein Isothionate-Dextran Product Information, 1997, pp. 1–3.

[29] M.L. Alessi, A.I. Norman, S.E. Knowlton, D.L. Ho, S.C. Greer, Helical and coil conformations of poly(ethylene glycol) in Isobutyric acid and water, Macromolecules 38 (22) (2005) 9333–9340, https://doi.org/10.1021/ma051339e.

[30] R.T. Robertson, S.T. Levine, S.M. Haynes, P. Gutierrez, J.L. Baratta, Z. Tan, K. J. Longmuir, Use of labeled tomato lectin for imaging vasculature structures, Histochem. Cell Biol. 143 (2) (2015) 225–234, https://doi.org/10.1007/s00418-014-1301-3.

[31] B. Bolon, Pathology Analysis of the Placenta, Elsevier, 2014, https://doi.org/10.1016/b978-0-12-394445-0.00014-x.

[32] S.A. Elmore, R.Z. Cochran, B. Bolon, B. Lubeck, B. Mahler, D. Sabio, J.M. Ward, Histology atlas of the developing mouse placenta, Toxicol. Pathol. 50 (1) (2022) 60–117, https://doi.org/10.1177/01926233211042270.

[33] G. Koren, G. Pariente, Pregnancy- associated changes in pharmacokinetics and their clinical implications, Pharm. Res. (2018) 35 (3), https://doi.org/10.1007/s11095-018-2352-2.

[34] M. Dawes, P.J. Chowienczyk, Pharmacokinetics in pregnancy, Best Pract. Res. Clin. Obstet. Gynaecol. 15 (6) (2001) 819–826, https://doi.org/10.1053/beog.2001.0231.

[35] M. Rothbauer, N. Patel, H. Gondola, M. Siwetz, B. Huppertz, P. Ertl, A comparative study of five physiological key parameters between four different human trophoblast-derived cell lines, Sci. Rep. 7 (1) (2017) 1–11, https://doi.org/10.1038/s41598-017-06364-z.

[36] X. Shao, G. Cao, D. Chen, J. Liu, B. Yu, M. Liu, Y.X. Li, B. Cao, Y. Sadovsky, Y. L. Wang, Placental trophoblast Syncytialization potentiates macropinocytosis via MTOR signaling to adapt to reduced amino acid supply, Proc. Natl. Acad. Sci. U. S. A. (2021) 118 (3), https://doi.org/10.1073/pnas.2017092118.

[37] L. Li, T. Wan, M. Wan, B. Liu, R. Cheng, R. Zhang, The effect of the size of fluorescent Dextran on its endocytic pathway, Cell Biol. Int. 39 (5) (2015) 531–539, https://doi.org/10.1002/cbin.10424.

[38] A. Schmidt, A. Schmidt, U.R. Markert, The road (not) taken – placental transfer and interspecies differences, The Road Not Taken. Placenta 115 (September) (2021) 70–77, https://doi.org/10.1016/j.placenta.2021.09.011.

[39] S.R. Sooranna, E. Oteng-Ntim, R. Meah, T.A. Ryder, R. Bajoria, Characterization of human placental explants: morphological, biochemical and physiological studies using first and third trimester placenta, Hum. Reprod. 14 (2) (1999) 536–541, https://doi.org/10.1093/humrep/14.2.536.

[40] Y. Qi, A. Chilkoti, Protein-polymer conjugation-moving beyond PEGylation, Curr. Opin. Chem. Biol. 28 (2015) 181–193, https://doi.org/10.1016/j.cbpa.2015.08.009.

[41] M. Zhu, A.K. Whittaker, F.Y. Han, M.T. Smith, Journey to the market: the evolution of biodegradable drug delivery systems, Appl. Sci. 12 (2) (2022), https://doi.org/10.3390/app12020935.